

Utility Analysis and Enhancement of LDP Mechanisms in High-Dimensional Space

Jiawei Duan^{* †}, Qingqing Ye^{*}, Haibo Hu^{*}

^{*} The Hong Kong Polytechnic University

[†] Centre for Advances in Reliability and Safety

jiawei.duan@connect.polyu.hk; qqing.ye@polyu.edu.hk; haibo.hu@polyu.edu.hk

Abstract—Local differential privacy (LDP), which perturbs each user’s data locally and only sends the noisy version of her information to the aggregator, is a popular privacy-preserving data collection mechanism. In LDP, the data collector could obtain accurate statistics without access to original data, thus guaranteeing users’ privacy. However, a primary drawback of LDP is its disappointing utility in high-dimensional space. Although various LDP schemes have been proposed to reduce perturbation, they share the same and naive aggregation mechanism at the collector’s side. In this paper, we first bring forward an analytical framework to generally measure the utilities of LDP mechanisms in high-dimensional space, which can benchmark existing and future LDP mechanisms without conducting any experiment. Based on this, the framework further reveals that the naive aggregation is sub-optimal in high-dimensional space, and there is much room for improvement. Motivated by this, we present a re-calibration protocol *HDR4ME* for high-dimensional mean estimation, which improves the utilities of existing LDP mechanisms without making any change to them. Both theoretical analysis and extensive experiments confirm the generality and effectiveness of our framework and protocol.

Index Terms—Local differential privacy, high-dimensional data, a general framework, regularization, proximal gradient descent

I. INTRODUCTION

In recent years, with growing number of IoT and smart devices, a huge amount of data becomes more accessible than ever [1]–[5]. Thanks to the advancement of modern machine learning and deep learning technologies, service providers and researchers nowadays can get insight into users’ behavior and intention with simple clicks. However, together with the prevalence of these technologies emerge privacy concerns during the collection of sensitive data about users. To balance data utility and privacy disclosure, an effective and highly recognized solution is local differential privacy (LDP) [6]–[8], where the data collector only collects perturbed data from users.

Nevertheless, existing LDP mechanisms mostly focus on low-dimensional data, mainly because the statistics estimated in high-dimensional space have low accuracy. As users only authorize a limited privacy budget to the collector, the allocated privacy budget in each dimension is diluted as the number of dimensions increases, which leads to more information loss and poorer statistics accuracy. Although much attention has been paid to develop less perturbed LDP mechanisms for

multi-dimensional data [9]–[12], they are still not applicable in high-dimensional space.

In this paper, we first propose an analytical framework that generalizes LDP mechanisms and derives their utilities in high-dimensional space, namely the probability density function of the deviation between the estimated mean and the true mean. The framework can serve as a benchmark to compare the utilities of various LDP mechanisms without conducting any experiment. Furthermore, our analysis shows the sub-optimality of the naive aggregation method of all LDP mechanisms — the utility deterioration is attributed to the overwhelming noise caused by diluted privacy budget in high-dimensional space. As such, our second contribution in this paper is a one-off, non-iterative re-calibration protocol *HDR4ME* (acronym for High-Dimensional Re-calibration for Mean Estimation). Through regularization and proximal gradient descent, this protocol re-calibrates the aggregated mean obtained from any LDP mechanism by suppressing the overwhelming noise and thus enhances its utility. Without any change on the LDP mechanism itself, *HDR4ME* can be used as a general optimizer of existing LDP mechanisms in high-dimensional space. In summary, our main contributions are:

- We bring forward an analytical framework to measure the utilities of LDP mechanisms in high-dimensional space. This framework not only provides a theoretical baseline to benchmark existing and future LDP mechanisms, but also serves as a platform to compare their theoretical utilities in high-dimensional space.
- We propose a re-calibration protocol *HDR4ME* to enhance high-dimensional mean estimation and prove its superiority to the baseline. In particular, this protocol can be further extended to frequency estimation.
- Based on both synthetic and real datasets, we conduct extensive experiments to validate our framework and evaluate our protocol for three state-of-the-art high-dimensional LDP mechanisms. Results show that the theoretical benchmark is consistent with the experimental results, and our protocol generally enhances the utilities.

The rest of this paper is organized as follows. In Section II, we review the related literature. Section III introduces the fundamental concepts and formulates the problem. Then we introduce the analytical framework for high-dimensional LDP

mechanisms in Section IV and propose our mean estimation protocol in Section V. Extensive experimental results are demonstrated in Section VI, and conclusions are made in Section VII.

II. RELATED WORK

Dwork *et al.* [13] formally present the definition of *differential privacy* (DP) and propose the first DP mechanism, i.e., *Laplace mechanism*. As for the local setting, Evfimievski *et al.* [14] are among the first to introduce differential privacy at the side of individuals. Then Raskhodnikova *et al.* [6] design a locally private mechanism γ -*amplification randomizer*. Later on, Duchi *et al.* [7] study the trade-off between local privacy budget and estimation utility, and derive bounds for *local differential privacy* (LDP). LDP has been widely adopted in different domains, including itemset mining [15], marginal release [16], [17], time series data release [18], graph data analysis [19]–[21], key-value data collection [22]–[24] and private learning [25], [26]. The most relevant problems to this paper include two aspects, namely, mean estimation by LDP and high-dimensional LDP.

A. Mean Estimation by LDP

Dwork *et al.* [13] initially propose *Laplace mechanism* for mean estimation for centralized DP, which can also be applied to the local setting. Afterwards, several LDP frameworks, such as a variant of *Laplace mechanism* referred to as *SCDF* [9] and *Staircase mechanism* [10], perturb values with less noise. Note that the perturbed values of these mechanisms range from negative to positive infinity, so they are classified as *unbounded mechanisms* in this paper. On the contrary, *bounded mechanisms* perturb values into a finite domain. Duchi *et al.* [27] present one whose outputs are binary. To overcome the shortcoming of binary output, Wang *et al.* [11] propose *Piecewise mechanism* and *Hybird mechanism*. With continuous and bounded outputs, their utilities are improved. More recently, Li *et al.* [12] propose *square wave mechanism* where the perturbation is more centered than Piecewise, and the utility is therefore superior.

B. High-Dimensional LDP

The most critical challenge to adopt LDP in high-dimensional space is the utility degradation, a.k.a., the dimensionality curse. In general, there are two streams of methodology to cope with it. One is dimensionality reduction. As for non-local privacy data publication, Ren *et al.* [28] study frequency estimation based on *Lasso Regression* and *EM* algorithm. By *principal components analysis* (PCA), Ge *et al.* [29] propose *DPS-PCA* for interactive LDP while Wang *et al.* [30] consider PCA for non-interactive LDP. Besides, Bassily [31] studies linear queries estimation in high-dimensional LDP. The other methodology is correlation-based privacy budget allocation. Chatzikokolakis *et al.* [32] use metric d_h to measure the similarity between two dimensions in DP. Larger d_h indicates lower similarity, which requires more privacy budget in those dimensions. Alvim *et al.* [33] extend this metric to LDP.

TABLE I
NOTATIONS

Symbol	Meaning
n	number of users
d	number of dimensions
\mathcal{M}	perturbation mechanism
\mathbf{t}_i	user's private tuple
\mathbf{t}_i^*	user's perturbed tuple
m	number of sampled dimensions
r	aggregator's received reports
θ	original mean
$\hat{\theta}$	estimated mean
$\hat{\theta}^*$	enhanced mean
\mathcal{L}	loss function
\mathcal{R}	regularizer
λ^*	regularization term

Similarly, Li *et al.* [34] calculate the respective information entropy of all dimensions while Du *et al.* [35] use covariance of different dimensions to allocate privacy budget accordingly.

It is noteworthy that almost all these works have limited the application scope in specific scenarios. Furthermore, many solutions have high computational cost at the user side [27], [29], [30], [32], [33]. This work, on the other hand, enhances high-dimensional LDP mean estimation by only involving the data collector. In addition, it is a general optimization that is irrespective of the LDP mechanisms.

III. PRELIMINARIES AND PROBLEM DEFINITION

A. Local Differential Privacy

In LDP, let n denote the number of users and tuple \mathbf{t}_i ($1 \leq i \leq n$) denote the i -th user's private data. To ensure privacy, each tuple \mathbf{t}_i is locally perturbed into \mathbf{t}_i^* by a certain perturbation mechanism \mathcal{M} . Afterwards, only perturbed tuples $\{\mathbf{t}_i^* | 1 \leq i \leq n\}$ are sent to the data collector. Table I summarizes the notations used throughout this paper. Given privacy budget $\epsilon > 0$ which indicates the privacy protection level, ϵ -*local differential privacy* is formally defined as follows:

Definition 1. (ϵ -local differential privacy) *A randomized perturbation mechanism \mathcal{M} satisfies ϵ -local differential privacy if and only if for any pair of tuples $\mathbf{t}_i, \mathbf{t}_j$, the following inequality always holds:*

$$\frac{\Pr(\mathcal{M}(\mathbf{t}_i) = \mathbf{t}^*)}{\Pr(\mathcal{M}(\mathbf{t}_j) = \mathbf{t}^*)} \leq \exp(\epsilon) \quad (1)$$

In essence, LDP guarantees that given prior knowledge \mathbf{t}^* , it is unlikely for the data collector to identify the data source with high confidence. Privacy budget ϵ controls the trade-off between privacy protection level and utility. Lower privacy budget means stricter privacy preservation and therefore poorer utility.

B. Problem Definition

In high-dimensional settings, each \mathbf{t}_i consists of d numerical dimensions $t_{i1}, t_{i2}, \dots, t_{id}$. Without loss of generality, we focus on mean estimation throughout this paper and assume that the domain of any dimension ranges from $[-1, 1]$. Unless

otherwise specified, we respectively use $\mathbb{E}(\cdot)$ and $Var(\cdot)$ to denote the expectation and the variance of a random variable.

Mean Estimation. We follow a common and general approach for LDP mechanisms to support high-dimensional data [11], [27], [36], [37]. Given a total privacy budget ϵ , each user randomly reports m ($1 \leq m \leq d$) dimensions of her perturbed data to the collector, with budget ϵ/m allocated to each dimension so that ϵ -LDP still holds. Let r_j denote the number of reports that the data collector receives in the j -th dimension, and obviously $\mathbb{E}(r_i) = \frac{nm}{d}$ because randomly reporting m out of d dimensions from n users' data is statistically equal to reporting d dimensions from $\frac{nm}{d}$ users. The data collector aggregates and estimates the mean of the j -th dimensions as $\hat{\theta}_j = \frac{1}{r_j} \sum_{i=1}^{r_j} t_{ij}^*$, so the estimated d -dimensional mean is $\hat{\theta} = (\hat{\theta}_1, \hat{\theta}_2, \dots, \hat{\theta}_{d-1}, \hat{\theta}_d)^\top$. Note that the original mean of users is $\bar{\theta} = \frac{1}{n} \sum_{i=1}^n t_i$. Our objective is for the estimated mean $\hat{\theta}$ to be as close to the original mean $\bar{\theta}$ as possible. Therefore, we adopt the following utility metrics which can measure their difference.

Utility Metrics. Theoretically, their difference can be measured by the *Euclidean distance*, i.e.,

$$\|\hat{\theta} - \bar{\theta}\|_2 = \sqrt{\sum_{j=1}^d |\hat{\theta}_j - \bar{\theta}_j|^2} \quad (2)$$

Following [11]–[13], we adopt *mean square error* (MSE) to measure experimental error, namely, the average squared difference between estimated means and original means over all dimensions, i.e.,

$$MSE(\hat{\theta}) = \frac{1}{d} \sum_{j=1}^d |\hat{\theta}_j - \bar{\theta}_j|^2 \quad (3)$$

Applying Equation 2 to Equation 3, we have $MSE(\hat{\theta}) = \frac{1}{d} \|\hat{\theta} - \bar{\theta}\|_2^2$, which means that the theoretical analysis on $\|\hat{\theta} - \bar{\theta}\|_2$ can predict how MSE varies without conducting any experiment.

In the rest of this paper, we focus on two tasks for mean estimation. First, we analyze the utilities of various LDP mechanisms when they are extended to high-dimensional space (see Section IV). Second, we design a re-calibration protocol to enhance the utility of any LDP mechanism in high-dimensional space without modifying it (see Section V).

IV. AN ANALYTICAL FRAMEWORK FOR HIGH-DIMENSIONAL LDP

In LDP literature, there are a lot of mechanisms that work in high-dimensional space. While a few are originally designed for such space [27], many others are extended or adapted to work in high-dimensional settings [9]–[13]. However, there is no theoretical work on benchmarking their utilities in high-dimensional space using a unified yardstick, based on which theoretical comparison and enhancement can be carried out. In this section, we provide such an analytical framework on **mean estimation** to better understand the theoretical performance

of existing works. Section IV-A first reviews three state-of-the-art LDP mechanisms, based on which we present our framework in Section IV-B. Section IV-C provides a case study on benchmarking Piecewise mechanism [11] and Square wave mechanism [12], and Section IV-D provides the convergence rate of our framework. Without loss of generality, in what follows we assume each dimension has a normalized value domain $[-1, 1]$, and some sampling techniques [11], [36], [37] are adopted so that each user only reports m out of d dimensions of her perturbed data to the data collector.

A. Three State-of-the-Art High-Dimensional LDP Mechanisms

Laplace mechanism. As a classic LDP mechanism, the advantage of *Laplace mechanism* [13] is its simplicity. Given that a one-dimensional value t_i in the range of $[-1, 1]$, the perturbed value $t_i^* = t_i + Lap(2/\epsilon)$, where $Lap(\lambda)$ denotes a random variable that follows Laplace distribution with probability density function $f(x) = \frac{1}{2\lambda} \exp(-\frac{|x|}{\lambda})$. Note that the variance of $Lap(\lambda)$ is $2\lambda^2$ [38]. To extend it to high-dimensional values, each dimension is perturbed independently with a random variable $Lap(2m/\epsilon)$ to guarantee ϵ -LDP. Since Laplace noise has zero mean, the data collector only needs to average all received tuples to achieve an unbiased mean estimation.

Generally, Laplace mechanism represents a class of LDP mechanisms [9], [10], [13] where the noise added to the original value ranges from negative to positive infinity. In our analytical framework, they are referred to as “unbounded mechanisms”.

Piecewise mechanism. In one-dimensional Piecewise mechanism [11], the perturbed value t^* of an original value $t \in [-1, 1]$ follows the distribution below:

$$\Pr(t^*) = \begin{cases} \frac{e^\epsilon - e^{-\epsilon/2}}{2e^{\epsilon/2} + 2} & t^* \in [l(t), r(t)] \\ \frac{1 - e^{-\epsilon/2}}{2e^{\epsilon/2} + 2} & t^* \in [-Q, l(t)) \cup (r(t), Q] \end{cases}, \quad (4)$$

where

$$Q = \frac{e^\epsilon + e^{\epsilon/2}}{e^\epsilon - e^{\epsilon/2}}$$

$$l(t) = \frac{Q+1}{2}t - \frac{Q-1}{2}$$

$$r(t) = l(t) + Q - 1$$

In high-dimensional space, similar to Laplace mechanism, each reporting dimension independently carries out ϵ/m -LDP. In contrast to Laplace mechanism, Piecewise mechanism perturbs the original value into a bounded domain $[-Q, Q]$, so such mechanisms are referred to as “bounded mechanisms”.

Square wave mechanism. This is yet another “bounded” LDP mechanism that improves Piecewise with more concentrated perturbation [12]. In its one-dimensional form, for any original value $t \in [0, 1]$, the perturbed value $t^* \in [-b, b+1]$ follows the distribution as below:

$$\Pr(t^*) = \begin{cases} \frac{e^\epsilon}{2be^\epsilon + 1} & \text{if } |t - t^*| < b \\ \frac{1}{2be^\epsilon + 1} & \text{otherwise} \end{cases}, \quad (5)$$

where $b = \frac{\epsilon e^\epsilon - e^\epsilon + 1}{2e^\epsilon(e^\epsilon - 1 - \epsilon)}$. Similar to Piecewise mechanism, in high-dimensional space, each reporting dimension carries out ϵ/m -LDP perturbation.

B. A General Analytical Framework

In this subsection, we present our general framework for high-dimensional LDP mechanisms. As aforementioned, we first use a boolean *Bound* to denote whether the perturbation of a certain LDP mechanism \mathcal{M} has a finite ‘‘boundary’’ B . Then a d -dimensional LDP mechanism with privacy budget ϵ is generalized as follows:

- 1) *Perturbation*: Each user has a private tuple \mathbf{t}_i ($1 \leq i \leq n$), among which m dimensional values are perturbed and reported. For each dimension j ($1 \leq j \leq d$), the mechanism obfuscates t_{ij} to t_{ij}^* with budget ϵ/m . If $\text{Bound}(\mathcal{M}) = 1$, the perturbed tuple satisfies $\mathbf{t}_i^* = \mathcal{M}(\mathbf{t}_i) \in [-B, B]^d$, where B is a both positive and finite value. Otherwise, the perturbed tuple satisfies $\mathbf{t}_i^* = \mathcal{M}(\mathbf{t}_i) = \mathbf{t}_i + \mathbf{N}_i$, where \mathbf{N}_i denotes a random tuple from \mathbb{R}^d .
- 2) *Calibration*: In each dimension j , the data collector receives r_j reports, where $r = \mathbb{E}(r_j) = \frac{nm}{d}$. Letting δ_{ij} denote the bias of $\mathbb{E}(t_{ij}^*)$, we have $\delta_{ij} = \mathbb{E}(t_{ij}^* - t_{ij})$. Accordingly, the collector calibrates the perturbed values by δ_{ij} . Note that $\delta_{ij} = 0$ carries out unbiased estimation.
- 3) *Aggregation*: For mean estimation in j -th dimension, the mechanism averages all calibrated values to obtain the estimated mean $\hat{\theta}_j = \frac{1}{r_j} \sum_{i=1}^{r_j} t_{ij}^*$.

Under this framework, we analyze the utility of high-dimensional LDP mechanisms based on the theoretical distance between the original mean $\bar{\theta}$ and the estimated mean $\hat{\theta}$ using *Lindeberg–Lévy Central Limit Theorem* (CLT) [39], [40]. Since each dimension is independently perturbed, we first model the deviation $\hat{\theta}_j - \bar{\theta}_j$ in one dimension.

Lemma 1. *For any \mathcal{M} and ϵ/m , $\text{Var}(t_{ij}^*)$ and δ_{ij} are deterministic if $\text{Bound}(\mathcal{M}) = 0$ while correlated to t_{ij} if $\text{Bound}(\mathcal{M}) = 1$.*

Proof. If $\text{Bound}(\mathcal{M}) = 0$, $\text{Var}(t_{ij}^*) = \text{Var}(t_{ij} + \mathbf{N}_{ij}) = \text{Var}(t_{ij}) + \text{Var}(\mathbf{N}_{ij}) = \text{Var}(\mathbf{N}_{ij})$ while $\delta_{ij} = \mathbb{E}(t_{ij}^* - t_{ij}) = \mathbb{E}(\mathbf{N}_{ij})$. Since \mathbf{N}_{ij} follows one perturbation, both $\text{Var}(t_{ij}^*)$ and δ_{ij} are deterministic. If $\text{Bound}(\mathcal{M}) = 1$, different t_{ij} correspond with different perturbations. Otherwise, t_{ij}^* would be totally independent from t_{ij} . In this case, $\text{Var}(t_{ij}^*)$ and δ_{ij} depend on t_{ij} . \square

Lemma 1 derives some common properties on $\text{Var}(t_{ij}^*)$ and δ_{ij} . Given \mathcal{M} and ϵ/m , $\text{Var}(t_{ij}^*)$ and δ_{ij} are certain functions of ϵ/m if $\text{Bound}(\mathcal{M}) = 0$. Otherwise, they are certain functions of both ϵ/m and t_{ij} . As long as the perturbation is known, we are able to provide $\text{Var}(t_{ij}^*)$ and δ_{ij} considering $\text{Var}(t_{ij}^*) = \mathbb{E}(t_{ij}^{*2}) - \mathbb{E}^2(t_{ij}^*)$ and $\delta_{ij} = \mathbb{E}(t_{ij}^* - t_{ij})$. For further utility analysis, we assume that $\text{Var}(t_{ij}^*)$ and δ_{ij} are already provided given certain \mathcal{M} and ϵ/m . Because

$\lim_{r_j \rightarrow \infty} \left(\frac{1}{r_j} \sum_{i=1}^{r_j} t_{ij} - \frac{1}{n} \sum_{i=1}^n t_{ij} \right) = 0$, the deviation $\hat{\theta}_j - \bar{\theta}_j$ can be simplified if $r_j \rightarrow \infty$:

$$\begin{aligned} \lim_{r_j \rightarrow \infty} \hat{\theta}_j - \bar{\theta}_j &= \lim_{r_j \rightarrow \infty} \left(\frac{1}{r_j} \sum_{i=1}^{r_j} t_{ij}^* - \frac{1}{n} \sum_{i=1}^n t_{ij} \right) \\ &= \lim_{r_j \rightarrow \infty} \left(\frac{1}{r_j} \sum_{i=1}^{r_j} t_{ij}^* - \frac{1}{r_j} \sum_{i=1}^{r_j} t_{ij} + \frac{1}{r_j} \sum_{i=1}^{r_j} t_{ij} - \frac{1}{n} \sum_{i=1}^n t_{ij} \right) \\ &= \lim_{r_j \rightarrow \infty} \frac{1}{r_j} \sum_{i=1}^{r_j} (t_{ij}^* - t_{ij}) \end{aligned} \quad (6)$$

Suppose that X is a random variable following standard normal distribution $X \sim \mathcal{N}(0, 1)$, and its probability density function is $\phi(x) = \frac{1}{\sqrt{2\pi}} \exp(-\frac{x^2}{2})$, the following two lemmas establish the asymptotic distribution of the deviation in one dimension.

Lemma 2. $\lim_{r_j \rightarrow \infty} \hat{\theta}_j - \bar{\theta}_j \sim \mathcal{N}\left(\mathbb{E}(\mathbf{N}_{ij}), \frac{\text{Var}(\mathbf{N}_{ij})}{r_j}\right)$, if $\text{Bound}(\mathcal{M}) = 0$.

Proof. For $\forall j$, $\{t_{ij}^* - t_{ij} | 1 \leq i \leq r_j\}$ are independent and identically distributed (i.i.d.) random variables because $t_{ij}^* - t_{ij} = \mathbf{N}_{ij}$. According to *Lindeberg–Lévy Central Limit Theorem* [39], [40], the following probability holds:

$$\begin{aligned} \lim_{r_j \rightarrow \infty} \Pr \left(\frac{\frac{1}{r_j} \sum_{i=1}^{r_j} (t_{ij}^* - t_{ij}) - \mathbb{E}(t_{ij}^* - t_{ij})}{\sqrt{\text{Var}(t_{ij}^* - t_{ij})/r_j}} \leq X \right) \\ = \lim_{r_j \rightarrow \infty} \Pr \left(\frac{\hat{\theta}_j - \bar{\theta}_j - \mathbb{E}(\mathbf{N}_{ij})}{\sqrt{\text{Var}(\mathbf{N}_{ij})/r_j}} \leq X \right) \\ = \int_{-\infty}^X \phi(x) dx \end{aligned} \quad (7)$$

Thus, $\lim_{r_j \rightarrow \infty} \frac{\hat{\theta}_j - \bar{\theta}_j - \mathbb{E}(\mathbf{N}_{ij})}{\sqrt{\text{Var}(\mathbf{N}_{ij})/r_j}}$ follows standard normal distribution $\mathcal{N}(0, 1)$, by which our claim is proven. \square

In Lemma 1, both $\text{Var}(t_{ij}^*) = \text{Var}(\mathbf{N}_{ij})$ and $\delta_{ij} = \mathbb{E}(\mathbf{N}_{ij})$ are deterministic if $\text{Bound}(\mathcal{M}) = 0$. On this basis, we could approximate $\hat{\theta}_j - \bar{\theta}_j$ using a specific Gaussian distribution $\mathcal{N}(\mathbb{E}(\mathbf{N}_{ij}), \text{Var}(\mathbf{N}_{ij})/r_j)$ if $\text{Bound}(\mathcal{M}) = 0$.

However, it is rather challenging if $\text{Bound}(\mathcal{M}) = 1$. Lemma 1 proves that different original values follow different perturbations if $\text{Bound}(\mathcal{M}) = 1$. Consequently, $\{t_{ij}^* - t_{ij} | 1 \leq i \leq r_j\}$ are probably not identically distributed, which does not satisfy the prerequisite of CLT [39], [40].

Nevertheless, we are still able to use one Gaussian distribution to approximate the summation of elements in any particular subset $\{t_{ij}^* - t_{ij}\}$, where all original data have the same value, and therefore CLT can be applied. Note that $\{t_{ij}^* - t_{ij} | 1 \leq i \leq r_j\}$ can be divided into several particular subsets by different original values. Let $\{v_j | 1 \leq j \leq d\}$ denote numbers of different original values in each dimension, $\{\mathbf{p}_{zj} | \sum_{z=1}^{v_j} \mathbf{p}_{zj} = 1\}$ denote their corresponding probabilities. As regards original data following continuous distri-

bution, we discretize them with sampling. The following lemma establishes the asymptotic distribution of the deviation in one dimension if $Bound(\mathcal{M}) = 1$, where we assume $\{\mathbf{t}_{ij}^* | 1 \leq i \leq r_j, 1 \leq j \leq d\}$ is in ascending order in each dimension.

Lemma 3. $\lim_{r_j \rightarrow \infty} \hat{\theta}_j - \bar{\theta}_j \sim \mathcal{N}\left(\mathbb{E}(\delta_{ij}), \frac{\mathbb{E}(Var(\mathbf{t}_{ij}^*))}{r_j}\right)$, where $\mathbb{E}(\delta_{ij}) = \sum_{z=1}^{v_j} \mathbf{p}_{zj} \delta_{(\sum_{o=1}^z r_j \mathbf{p}_{oj})j}$ and $\mathbb{E}(Var(\mathbf{t}_{ij}^*)) = \sum_{z=1}^{v_j} \mathbf{p}_{zj} Var(\mathbf{t}_{(\sum_{o=1}^z r_j \mathbf{p}_{oj})j}^*)$, if $Bound(\mathcal{M}) = 1$.

Proof. For $1 \leq c \leq v_j$, the original data in $\{\mathbf{t}_{ij}^* | r_j \sum_{z=1}^{c-1} \mathbf{p}_{zj} < i \leq r_j \sum_{z=1}^c \mathbf{p}_{zj}\}$ share the same value. Therefore, $\{\mathbf{t}_{ij}^* - \mathbf{t}_{ij} | r_j \sum_{z=1}^{c-1} \mathbf{p}_{zj} < i \leq r_j \sum_{z=1}^c \mathbf{p}_{zj}\}$ are i.i.d. random variables. According to *Lindeberg–Lévy Central Limit Theorem* [39], [40], the following probability holds if r_j approaches ∞ :

$$\begin{aligned} & \Pr\left(\frac{\sum_{i=r_j \sum_{z=1}^{c-1} \mathbf{p}_{zj} + 1}^{r_j \sum_{z=1}^c \mathbf{p}_{zj}} (\mathbf{t}_{ij}^* - \mathbf{t}_{ij} - \mathbb{E}(\mathbf{t}_{ij}^* - \mathbf{t}_{ij}))}{\sqrt{Var(\mathbf{t}_{ij}^* - \mathbf{t}_{ij}) r_j \mathbf{p}_{cj}}} \leq X\right) \\ &= \Pr\left(\frac{\sum_{i=r_j \sum_{z=1}^{c-1} \mathbf{p}_{zj} + 1}^{r_j \sum_{z=1}^c \mathbf{p}_{zj}} (\mathbf{t}_{ij}^* - \mathbf{t}_{ij} - \delta_{ij})}{\sqrt{Var(\mathbf{t}_{ij}^*) r_j \mathbf{p}_{cj}}} \leq X\right) \\ &= \int_{-\infty}^X \phi(x) dx \end{aligned} \quad (8)$$

Therefore, $\frac{\sum_{i=r_j \sum_{z=1}^{c-1} \mathbf{p}_{zj} + 1}^{r_j \sum_{z=1}^c \mathbf{p}_{zj}} (\mathbf{t}_{ij}^* - \mathbf{t}_{ij} - \delta_{ij})}{\sqrt{Var(\mathbf{t}_{ij}^*) r_j \mathbf{p}_{cj}}}$ approximately follows standard normal distribution $\mathcal{N}(0, 1)$. Next, we use *Mathematical Induction* to complete the proof.

For $c = 1$, Equation 8 establishes $\sum_{i=1}^{r_j \mathbf{p}_{1j}} (\mathbf{t}_{ij}^* - \mathbf{t}_{ij} - \delta_{ij}) \sim \mathcal{N}(0, r_j \mathbf{p}_{1j} Var(\mathbf{t}_{(r_j \mathbf{p}_{1j})j}^*))$.

Suppose that $\sum_{i=1}^{r_j \sum_{z=1}^c \mathbf{p}_{zj}} (\mathbf{t}_{ij}^* - \mathbf{t}_{ij} - \delta_{ij}) \sim \mathcal{N}(0, \sum_{z=1}^c r_j \mathbf{p}_{zj} Var(\mathbf{t}_{(\sum_{o=1}^z r_j \mathbf{p}_{oj})j}^*))$ holds for $1 < c < v_j$, we have the following for $r_j \rightarrow \infty$:

$$\begin{aligned} \sum_{i=1}^{r_j \sum_{z=1}^{c+1} \mathbf{p}_{zj}} (\mathbf{t}_{ij}^* - \mathbf{t}_{ij} - \delta_{ij}) &= \sum_{i=1}^{r_j \sum_{z=1}^c \mathbf{p}_{zj}} (\mathbf{t}_{ij}^* - \mathbf{t}_{ij} - \delta_{ij}) \\ &+ \sum_{i=r_j \sum_{z=1}^c \mathbf{p}_{zj} + 1}^{r_j \sum_{z=1}^{c+1} \mathbf{p}_{zj}} (\mathbf{t}_{ij}^* - \mathbf{t}_{ij} - \delta_{ij}) \end{aligned} \quad (9)$$

According to Equation 8, $\sum_{i=r_j \sum_{z=1}^c \mathbf{p}_{zj} + 1}^{r_j \sum_{z=1}^{c+1} \mathbf{p}_{zj}} (\mathbf{t}_{ij}^* - \mathbf{t}_{ij} - \delta_{ij})$ follows $\mathcal{N}(0, r_j \mathbf{p}_{(c+1)j} Var(\mathbf{t}_{(r_j \mathbf{p}_{(c+1)j})j}^*))$. Given $Y \sim \mathcal{N}(\mu_1, \sigma_1^2)$ and $Z \sim \mathcal{N}(\mu_2, \sigma_2^2)$, $Y + Z \sim \mathcal{N}(\mu_1 + \mu_2, \sigma_1^2 + \sigma_2^2)$ [41]. Therefore, we prove that for $1 < c < v_j$ and $r_j \rightarrow \infty$,

$$\begin{aligned} & \sum_{i=1}^{r_j \sum_{z=1}^{c+1} \mathbf{p}_{zj}} (\mathbf{t}_{ij}^* - \mathbf{t}_{ij} - \delta_{ij}) \\ & \sim \mathcal{N}\left(0, \sum_{z=1}^{c+1} r_j \mathbf{p}_{zj} Var(\mathbf{t}_{(\sum_{o=1}^z r_j \mathbf{p}_{oj})j}^*)\right) \end{aligned} \quad (10)$$

Letting $c = v_j - 1$, if r_j approaches ∞ , we have:

$$\begin{aligned} & \Pr\left(\frac{\hat{\theta}_j - \bar{\theta}_j - \mathbb{E}(\delta_{ij})}{\sqrt{\sum_{z=1}^{v_j} \mathbf{p}_{zj} Var(\mathbf{t}_{(\sum_{o=1}^z r_j \mathbf{p}_{oj})j}^*)} / r_j} \leq X\right) \\ &= \Pr\left(\frac{\sum_{i=1}^{r_j} (\mathbf{t}_{ij}^* - \mathbf{t}_{ij}) - \sum_{z=1}^{v_j} r_j \mathbf{p}_{zj} \delta_{(\sum_{o=1}^z r_j \mathbf{p}_{oj})j}}{\sqrt{\sum_{z=1}^{v_j} r_j \mathbf{p}_{zj} Var(\mathbf{t}_{(\sum_{o=1}^z r_j \mathbf{p}_{oj})j}^*)}} \leq X\right) \\ &= \Pr\left(\frac{\sum_{i=1}^{r_j} (\mathbf{t}_{ij}^* - \mathbf{t}_{ij} - \delta_{ij})}{\sqrt{\sum_{z=1}^{v_j} r_j \mathbf{p}_{zj} Var(\mathbf{t}_{(\sum_{o=1}^z r_j \mathbf{p}_{oj})j}^*)}} \leq X\right) \\ &= \int_{-\infty}^X \phi(x) dx \end{aligned} \quad (11)$$

by which our claim is proven. \square

Note that $\mathbb{E}(\delta_{ij})$ and $\mathbb{E}(Var(\mathbf{t}_{ij}^*))$ computes the expectations of δ_{ij} and $Var(\mathbf{t}_{ij}^*)$ in terms of \mathbf{t}_{ij}^* . In general, Lemma 2 and Lemma 3 establish that no matter how the original data is distributed, $\hat{\theta}_j - \bar{\theta}_j$ always approximates a normal distribution. However, its variance is split into two cases. If $Bound(\mathcal{M}) = 0$, it is only decided by the distribution of perturbation; otherwise, it is collectively decided by distributions of both perturbation and original data. As such, given a certain dataset and a budget, we can model how $\hat{\theta}_j - \bar{\theta}_j$ varies in terms of any mechanism.

What if multiple or even high dimensions? Note that each dimension is independently perturbed with privacy budget ϵ/m . As each dimension of the deviation approximates a one-dimensional normal distribution, we can model the deviation $\hat{\theta} - \bar{\theta}$ with one multivariate normal distribution. Following Lemma 2 or Lemma 3, for $1 \leq j \leq d$, $\hat{\theta}_j - \bar{\theta}_j$ approximates a normal distribution whose probability density function is $f(\hat{\theta}_j - \bar{\theta}_j) = \frac{1}{\sqrt{2\pi}\sigma_j} \exp(-\frac{(\hat{\theta}_j - \bar{\theta}_j - \delta_j)^2}{2\sigma_j^2})$. Then the following theorem models the deviation in high-dimensional space.

Theorem 1. For any high-dimensional LDP mechanism, the probability density function (pdf) of $\hat{\theta} - \bar{\theta}$ is:

$$\lim_{r \rightarrow \infty} f(\hat{\theta} - \bar{\theta}) = \frac{1}{(\sqrt{2\pi})^d \prod_{j=1}^d \sigma_j} \exp\left(-\sum_{j=1}^d \frac{(\hat{\theta}_j - \bar{\theta}_j - \delta_j)^2}{2\sigma_j^2}\right) \quad (12)$$

Proof. Since each dimension is perturbed independently, we have:

$$\begin{aligned} f(\hat{\theta} - \bar{\theta}) &= \prod_{j=1}^d f(\hat{\theta}_j - \bar{\theta}_j) = \prod_{j=1}^d \frac{1}{\sqrt{2\pi}\sigma_j} \exp\left(-\frac{(\hat{\theta}_j - \bar{\theta}_j - \delta_j)^2}{2\sigma_j^2}\right) \\ &= \frac{1}{(\sqrt{2\pi})^d \prod_{j=1}^d \sigma_j} \exp\left(-\sum_{j=1}^d \frac{(\hat{\theta}_j - \bar{\theta}_j - \delta_j)^2}{2\sigma_j^2}\right) \end{aligned} \quad (13)$$

As this pdf models how $\hat{\theta} - \bar{\theta}$ varies in high-dimensional space, we can accommodate almost all utility metrics for

comparisons, including the supremum of the deviation. To benchmark different LDP mechanisms, intuitively the smallest supremum of the deviation $\sup \|\hat{\theta} - \bar{\theta}\|_2$ should have the best utility. However, due to the randomness in LDP mechanisms, the absolute supremum can be infinity. As such, the data collector can manually specify the supremum of deviation she wants to tolerate, and then calculate the corresponding probability for that supremum to hold using this pdf. Let $\xi = (\xi_1, \dots, \xi_d)^\top = \left(\sup |\hat{\theta}_1 - \bar{\theta}_1|, \dots, \sup |\hat{\theta}_d - \bar{\theta}_d| \right)^\top$ denotes the supremum and $S = \left\{ \hat{\theta} - \bar{\theta} \in \mathbb{R}^d : \forall j, |\hat{\theta}_j - \bar{\theta}_j| \leq \xi_j \right\}$ denotes the subspace bounded by the supremum, then the integral of the pdf $\int_S f(\hat{\theta} - \bar{\theta}) d(\hat{\theta} - \bar{\theta})$ is the probability of the deviation within the supremum. Accordingly, the LDP mechanism with the highest probability is considered the best in high-dimensional space. Note that different supremum settings can lead to different winners. Next, we provide a case study to demonstrate how to benchmark Piecewise mechanism and Square wave mechanism by our framework.

C. A Case Study: How to Benchmark Piecewise Mechanism and Square Wave Mechanism in High-Dimensional Space?

Since each dimension is perturbed equivalently in high-dimensional space, we study how to benchmark these two mechanisms in any single dimension. Suppose an original dataset with $d = 100$ dimensions and $n = 10000$ users, there are $v = 10$ different original values $\{0.1, 0.2, 0.3, \dots, 0.8, 0.9, 1.0\}$ in each dimension. For simplicity, we presume that the corresponding probability of each value in each dimension is $p = 10\%$. For each user, she reports $m = 100$ dimensions of her data to the data collector. As such, the data collector receives $r = \frac{nm}{d} = 10000$ reports. Given the collective privacy budget $\epsilon = 0.1$, each dimension is allocated $\epsilon/m = 0.001$ privacy budget. Next, we demonstrate how to obtain the pdf in Theorem 1 for each LDP mechanism. For Piecewise mechanism, we first obtain the variance of t_{ij}^* :

$$\begin{aligned} Var(t_{ij}^*) &= \mathbb{E}(t_{ij}^{*2}) - \mathbb{E}^2(t_{ij}^*) \\ &= \int_{-Q}^{l(t_{ij}^*)} \frac{(1 - e^{-\epsilon/2m})x^2}{2e^{\epsilon/2m} + 2} dx \\ &\quad + \int_{l(t_{ij}^*)}^{r(t_{ij}^*)} \frac{(e^{\epsilon/m} - e^{\epsilon/2m})x^2}{2e^{\epsilon/2m} + 2} dx \\ &\quad + \int_{r(t_{ij}^*)}^Q \frac{(1 - e^{-\epsilon/2m})x^2}{2e^{\epsilon/2m} + 2} dx \\ &= \frac{t_{ij}^*}{e^{\epsilon/2m} - 1} + \frac{e^{\epsilon/2m+3}}{3(e^{\epsilon/2m} - 1)^2} \end{aligned} \quad (14)$$

We then derive the variance σ_j^2 of Gaussian distribution that approximates $\hat{\theta}_j - \bar{\theta}_j$ according to Lemma 3:

$$\begin{aligned} \sigma_j^2 &= \frac{\sum_{z=1}^v p Var(t_{\sum_{o=1}^z rp}^*)}{r} \\ &= \frac{10\% \times (0.1 + 0.2 + \dots + 1.0)}{e^{0.001/2} - 1} + \frac{e^{0.001/2+3}}{3(e^{0.001/2} - 1)^2} \\ &= 533.210 \end{aligned} \quad (15)$$

Due to unbiased estimation, we can derive the pdf of $\hat{\theta}_j - \bar{\theta}_j$ in Piecewise mechanism by applying $d = 1$, $\sigma_j^2 = 533.210$, and $\delta_j = 0$ to Equation 12:

$$f(\hat{\theta}_j - \bar{\theta}_j) = \frac{1}{57.900} \exp\left(-\frac{(\hat{\theta}_j - \bar{\theta}_j)^2}{1066.420}\right) \quad (16)$$

For the Square wave mechanism, we have the bias of $\mathbb{E}(t_{ij}^*)$:

$$\begin{aligned} \delta_{ij} &= \mathbb{E}(t_{ij}^* - t_{ij}) \\ &= \int_{-b}^{t_{ij}-b} \frac{x}{2be^{\epsilon/m} + 1} dx + \int_{t_{ij}-b}^{t_{ij}+b} \frac{x e^{\epsilon/m}}{2be^{\epsilon/m} + 1} dx \\ &\quad + \int_{t_{ij}+b}^{1+b} \frac{x}{2be^{\epsilon/m} + 1} dx - t_{ij} \\ &= \frac{2b(e^{\epsilon/m} - 1)t_{ij}}{2be^{\epsilon/m} + 1} + \frac{1 + 2b}{2(2be^{\epsilon/m} + 1)} - t_{ij} \end{aligned} \quad (17)$$

and the variance of t_{ij}^* :

$$\begin{aligned} Var(t_{ij}^*) &= \mathbb{E}(t_{ij}^{*2}) - \mathbb{E}^2(t_{ij}^*) \\ &= \int_{-b}^{t_{ij}-b} \frac{x^2}{2be^{\epsilon/m} + 1} dx + \int_{t_{ij}-b}^{t_{ij}+b} \frac{x^2 e^{\epsilon/m}}{2be^{\epsilon/m} + 1} dx \\ &\quad + \int_{t_{ij}+b}^{1+b} \frac{x^2}{2be^{\epsilon/m} + 1} dx - (t_{ij} + \delta_{ij})^2 \\ &= \frac{b^2}{3} + \frac{(2b+1)(b+1-3t_{ij}^2)}{3(2be^{\epsilon/m} + 1)} - \delta_{ij}^2 - 2\delta_{ij}t_{ij} \end{aligned} \quad (18)$$

We then derive the bias δ_j and the variance σ_j^2 of the Gaussian distribution that approximates $\hat{\theta}_j - \bar{\theta}_j$ according to Lemma 3:

$$\begin{aligned} \delta_j &= \sum_{z=1}^v p \delta_{ij} = -0.049 \\ \sigma_j^2 &= \frac{\sum_{z=1}^v p Var(t_{\sum_{o=1}^z rp}^*)}{r} = 3.365 \times 10^{-5} \end{aligned} \quad (19)$$

Finally, according to Theorem 1, we can derive the pdf of $\hat{\theta}_j - \bar{\theta}_j$ in the Square wave mechanism by applying Equation 19 and $d = 1$ to Equation 12:

$$f(\hat{\theta}_j - \bar{\theta}_j) = \frac{1}{0.015} \exp\left(-\frac{10^5(\hat{\theta}_j - \bar{\theta}_j + 0.049)^2}{6.730}\right) \quad (20)$$

Now that we have derived the pdf of $\hat{\theta}_j - \bar{\theta}_j$ in both LDP mechanisms, its integral $\int_{-\xi_j}^{\xi_j} f(\hat{\theta}_j - \bar{\theta}_j) d(\hat{\theta}_j - \bar{\theta}_j)$ is the probability that the deviation in j -th dimension is still within the supremum $\xi_j = \sup |\hat{\theta}_j - \bar{\theta}_j|$. The higher probability the better the LDP mechanism. We vary ξ_j from 0.001 to 0.1 and show the resulted probabilities in Table II. Piecewise mechanism is better than Square wave mechanism for smaller supremums (e.g., 0.001, 0.01), which is mainly because Piecewise is an unbiased estimation while Square wave is not. However, if the supremum becomes larger (e.g., 0.05, 0.1), in other words, if the collector can tolerate larger deviation, the Square wave mechanism is far better than the Piecewise mechanism because the variance of Gaussian distribution that approximates $\hat{\theta}_j - \bar{\theta}_j$

in the former is much smaller than that in the latter. That is to say, whether Piecewise or Square wave should be chosen depend on her tolerance of supremum ξ_j .

TABLE II
PROBABILITIES FOR THE SUPREMUM TO HOLD IN ONE DIMENSION

ξ_j	0.001	0.01	0.05	0.1
Piecewise	3.46×10^{-5}	3.46×10^{-4}	0.002	0.004
Square	2.12×10^{-16}	2.62×10^{-11}	0.644	1.000

D. Approximation Error of Theorem 1

Our analytical framework is based on one assumption that the data collector receives sufficiently large number of reports from users. Otherwise, the *central limit theorem* provides an asymptotic approximation of the deviation. In order to find the gap between the approximated deviation and the true one, we study the approximation error of $\hat{\theta}_j - \bar{\theta}_j$ in terms of the number of reports r_j . Suppose the true pdf of $\hat{\theta}_j - \bar{\theta}_j$ is \bar{f}_j , its corresponding cumulative distribution function (cdf) would be $\bar{F}_j(x) = \int_{-\infty}^x \bar{f}_j(\hat{\theta}_j - \bar{\theta}_j) d(\hat{\theta}_j - \bar{\theta}_j)$. According to Lemma 2 or Lemma 3, the approximated pdf of $\hat{\theta}_j - \bar{\theta}_j$ is $\hat{f}_j(\hat{\theta}_j - \bar{\theta}_j) = \frac{1}{\sqrt{2\pi}\sigma_j} \exp(-\frac{(\hat{\theta}_j - \bar{\theta}_j - \delta_{ij})^2}{2\sigma_j^2})$, and its corresponding cdf is $\hat{F}_j(x) = \int_{-\infty}^x \hat{f}_j(\hat{\theta}_j - \bar{\theta}_j) d(\hat{\theta}_j - \bar{\theta}_j)$. Then we have:

Theorem 2. For any LDP mechanism, the true cdf $\bar{F}_j(x)$ and the approximated cdf $\hat{F}_j(x)$ of $\hat{\theta}_j - \bar{\theta}_j$ differ by no more than $\frac{0.33554(\rho+0.415(r_j\sigma_j)^3)}{r_j^{7/2}\sigma_j^3}$, where $\rho = \mathbb{E}(|t_{ij}^* - t_{ij} - \delta_{ij}|^3)$.

Proof. As necessary prerequisites, $\mathbb{E}(t_{ij}^* - t_{ij} - \delta_{ij}) = 0$, and Lemma 2 and Lemma 3 prove that $\mathbb{E}((t_{ij}^* - t_{ij} - \delta_{ij})^2) = \mathbb{E}(\text{Var}(t_{ij}^* - t_{ij} - \delta_{ij}) + \mathbb{E}^2(t_{ij}^* - t_{ij} - \delta_{ij})) = \mathbb{E}(\text{Var}(t_{ij}^* - t_{ij} - \delta_{ij})) = \mathbb{E}(\text{Var}(t_{ij}^*)) = (r_j\sigma_j)^2$. Besides, we have to prove $\rho < \infty$. If $\text{Bound}(\mathcal{M}) = 1$, it surely establishes because t_{ij}^* , t_{ij} and δ_{ij} are all finite values in this case. If $\text{Bound}(\mathcal{M}) = 0$, we can prove that *Laplace mechanism* satisfies this term. Note that $t_{ij}^* - t_{ij} - \delta_{ij} = N_{ij}$. Therefore, we have:

$$\begin{aligned} \rho &= \mathbb{E}(|t_{ij}^* - t_{ij} - \delta_{ij}|^3) \\ &= \int_{-\infty}^{\infty} |x|^3 \text{Lap}(\lambda = 2m/\epsilon) dx \\ &= \frac{1}{\lambda} \int_0^{\infty} x^3 \exp(-\frac{x}{\lambda}) dx \\ &= \frac{3\lambda}{2} \mathbb{E}(x^2) = \frac{3\lambda}{2} 2\lambda^2 = 3\lambda^3 = \frac{24m^3}{\epsilon^3} \leq \infty \end{aligned} \quad (21)$$

As such, *Berry-Esseen theorem* [42] establishes:

$$\sup_{x \in \mathbb{R}} |\bar{F}_j(x) - \hat{F}_j(x)| \leq \frac{0.33554(\rho + 0.415(r_j\sigma_j)^3)}{r_j^{7/2}\sigma_j^3} \quad (22)$$

□

According to Lemma 2 and Lemma 3, the value of $r_j\sigma_j$ is irrelevant to r_j . Thus, $r_j\sigma_j$ can be taken as a fixed value, which implies that the speed of convergence rate in

our framework is at least on the order of $\frac{r_j^3}{r_j^{7/2}} = \frac{1}{\sqrt{r_j}}$. That is to say, the approximation error is still tolerable even if the number of reports is insufficient. We take *Laplace mechanism* for example, where $\rho = 3\lambda^3$ in Equation 21 and $r_j\sigma_j = \sqrt{\text{Var}(t_{ij}^*)} = \sqrt{(\text{Var}(\text{Lap}(\lambda)))} = \sqrt{2\lambda}$. Suppose the data collector only receives $r_j = 1000$ reports, the approximation error between the true cdf and the approximated cdf of $\hat{\theta}_j - \bar{\theta}_j$ is no more than $\frac{0.33554(\rho+0.415(r_j\sigma_j)^3)}{r_j^{7/2}\sigma_j^3} = \frac{0.33554 \times (3 \times \lambda^3 + 0.415 \times 2 \times \sqrt{2} \times \lambda^3)}{2 \times \sqrt{2} \times \lambda^3 \times \sqrt{r_j}} \approx 1.57\%$.

V. HDR4ME: HIGH-DIMENSIONAL RE-CALIBRATION FOR MEAN ESTIMATION

In our analytical framework, we observe that dimensions d has significant and direct influence on the deviation. In specific, d dictates the privacy budget in each dimension, which directly affects the accuracy. In this section, we seize this opportunity to reduce the effective d in the aggregation phase to improve the accuracy. The rationale of targeting at the aggregation phase instead of the perturbation or calibration is obvious — the latter are mechanism-dependent whereas the former is universal to all LDP mechanisms. As such, our enhancement is orthogonal to all existing LDP optimizations.

In what follows, we first introduce *regularization* that can mitigate the negative influence in high dimensions. By integrating it into the aggregation, we propose a *re-calibration protocol HDR4ME* and a solver algorithm based on proximal gradient descent. Last, we extend *HDR4ME* for frequency estimation. Rigorous analysis is provided to prove its superiority over the existing one.

A. Regularization: Diminishing Utility Deterioration in High-dimensional Space

Regularization is a common technique to re-calibrate the minimization tasks [43]–[47]. On the one hand, it directly reduces the dimensions d . On the other hand, it also reduces the scale of the perturbed data and thus diminishes the variance, which counteracts the utility deterioration caused by high dimensionality [27].

To explain regularization, let $\mathcal{L}(\theta)$ denote a certain loss function regarding $\theta \in \mathbb{R}^d$ while the regularization term is $\mathcal{R}(\theta)$. $\mathcal{R}(\theta) = \|\theta\|_1$ and $\mathcal{R} = \|\theta\|_2$ are the operators for L_1 -regularization (abbreviated as L_1) and L_2 -regularization (abbreviated as L_2), respectively. Figure 1 illustrates the physical meaning of both regularizations in two dimensional space, where the black curves are isopleths of any loss function $\mathcal{L}(\theta)$. The red square is the shape of L_1 , while the blue circle is the shape of L_2 . We notice that $\mathcal{L}(\theta)$ converges to $\hat{\theta}$ without regularization. In contrast to $\hat{\theta}$, $\mathcal{L}(\theta)$ tends to cross on coordinate axes with L_1 while it tends to cross on the circle with L_2 . Let θ^* denote the regularized results. Comparing both θ^* with $\hat{\theta}$, L_1 reduces both dimensions and the scale of $\hat{\theta}$ while L_2 just reduces the scale of $\hat{\theta}$. By integrating them in the aggregation phase as a re-calibration, we can mitigate the negative influence by high dimensionality. In

the next subsection, we propose our re-calibration protocol *HDR4ME*.

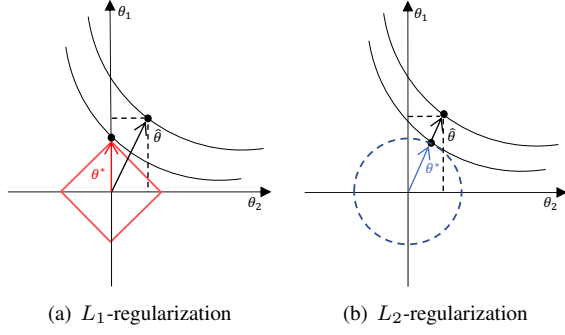


Fig. 1. Regularization in two dimensions.

B. HDR4ME—High Dimensional Re-calibration for Mean Estimation

Recall that in each dimension, the data collector receives r perturbed tuples $\{\mathbf{t}_i^* | 1 \leq i \leq r\}$, where $r = \frac{nm}{d}$. To add regularization terms, we first define the loss function of the aggregation $\mathcal{L}(\boldsymbol{\theta}) = \frac{1}{2r} \sum_{i=1}^r \|\mathbf{t}_i^* - \boldsymbol{\theta}\|_2^2$. On this basis, we add regularization terms $\mathcal{R}(\boldsymbol{\theta})$ to $\mathcal{L}(\boldsymbol{\theta})$ to obtain the enhanced mean $\boldsymbol{\theta}^*$ as follows:

$$\boldsymbol{\theta}^* = \arg \min_{\boldsymbol{\theta} \in \mathbb{R}^d} \{\mathcal{L}(\boldsymbol{\theta}) + \mathcal{R}(\boldsymbol{\lambda}^* \circ \boldsymbol{\theta})\}, \quad (23)$$

where $\mathcal{R}(\boldsymbol{\theta}) = \|\boldsymbol{\theta}\|_1$ or $\|\boldsymbol{\theta}\|_2$ and $\boldsymbol{\lambda}^* = (\lambda_1^*, \dots, \lambda_d^*)^\top$ is the regularization weight (which controls the degree of the involvement of regularization). In particular, $\boldsymbol{\lambda}^* \circ \boldsymbol{\theta} = (\lambda_1^* \theta_1, \dots, \lambda_d^* \theta_d)^\top$ is *Hadamard product*. In what follows, we provide detailed utility analysis of *HDR4ME* with L_1 - and L_2 -regularization, respectively, together with the specification of $\boldsymbol{\lambda}^*$.

HDR4ME with L_1 -regularization. With this re-calibration, the deviation $\|\hat{\boldsymbol{\theta}} - \bar{\boldsymbol{\theta}}\|_2$ can be significantly reduced by dimensionality and perturbation reduction. The following lemma discusses the suitable choice of $\boldsymbol{\lambda}^*$ and the threshold for utility enhancement.

Lemma 4. *HDR4ME with L_1 -regularization can improve accuracy in j -th dimension if*

$$\lambda_j^* = \sup |\hat{\boldsymbol{\theta}}_j - \bar{\boldsymbol{\theta}}_j| \text{ and } |\hat{\boldsymbol{\theta}}_j - \bar{\boldsymbol{\theta}}_j| > 1 \quad (24)$$

where $\hat{\boldsymbol{\theta}}_j - \bar{\boldsymbol{\theta}}_j$ is obtained from Lemma 2 or Lemma 3.

Proof. Since $\|\boldsymbol{\theta}\|_1$ is non-differentiable, we adopt an alternative solution, namely, proximal gradient descent (PGD) [43], [48], [49]. Our objective is to obtain the iterative equation to solve our protocol. First, we get the derivative of $\mathcal{L}(\boldsymbol{\theta})$:

$$\nabla \mathcal{L}(\boldsymbol{\theta}) = \frac{1}{r} \sum_{i=1}^r (\boldsymbol{\theta} - \mathbf{t}_i^*) = \boldsymbol{\theta} - \frac{1}{r} \sum_{i=1}^r \mathbf{t}_i^* = \boldsymbol{\theta} - \hat{\boldsymbol{\theta}} \quad (25)$$

Thus, the derivative of $\nabla \mathcal{L}(\boldsymbol{\theta})$ is $\frac{d \nabla \mathcal{L}(\boldsymbol{\theta})}{d \boldsymbol{\theta}} = 1$. According to *Cauchy mean value theorem*, we have:

$$\|\nabla \mathcal{L}(\boldsymbol{\theta}) - \nabla \mathcal{L}(\boldsymbol{\theta}_k)\|_2^2 \leq \|\boldsymbol{\theta} - \boldsymbol{\theta}_k\|_2^2, \quad (26)$$

where $\boldsymbol{\theta}_k$ is the result of k -th iteration. By *second-order Taylor expansion* around $\boldsymbol{\theta}_k$, we get:

$$\begin{aligned} \mathcal{L}(\boldsymbol{\theta}) &\cong \mathcal{L}(\boldsymbol{\theta}_k) + \langle \nabla \mathcal{L}(\boldsymbol{\theta}_k), \boldsymbol{\theta} - \boldsymbol{\theta}_k \rangle + \frac{1}{2} \|\boldsymbol{\theta} - \boldsymbol{\theta}_k\|_2^2 \\ &= \frac{1}{2} \|\boldsymbol{\theta} - (\boldsymbol{\theta}_k - \nabla \mathcal{L}(\boldsymbol{\theta}_k))\|_2^2 + \text{constant} \end{aligned} \quad (27)$$

To minimize the loss function \mathcal{L} , we get the iterative equation $\boldsymbol{\theta}_{k+1} = \boldsymbol{\theta}_k - \nabla \mathcal{L}(\boldsymbol{\theta}_k)$. We then introduce L_1 -regularization term into the iteration:

$$\boldsymbol{\theta}_{k+1} = \arg \min_{\boldsymbol{\theta}} \frac{1}{2} \|\boldsymbol{\theta} - (\boldsymbol{\theta}_k - \nabla \mathcal{L}(\boldsymbol{\theta}_k))\|_2^2 + \|\boldsymbol{\lambda}^* \circ \boldsymbol{\theta}\|_1 \quad (28)$$

Since each dimension is independent of each other, we have the following solution for each dimension:

$$(\boldsymbol{\theta}_{k+1})_j = \arg \min_{\theta_j} \frac{1}{2} |\theta_j - ((\boldsymbol{\theta}_k)_j - \nabla \mathcal{L}(\boldsymbol{\theta}_k)_j)|_2^2 + |\lambda_j^* \theta_j|_1 \quad (29)$$

As such, how to compute $(\boldsymbol{\theta}_{k+1})_j$ really depends on whether $\boldsymbol{\theta}_j$ is positive, zero or negative (λ_j^* is positive). In particular, we let $\mathbf{z} = \boldsymbol{\theta}_k - \nabla \mathcal{L}(\boldsymbol{\theta}_k) = \boldsymbol{\theta}_k - \boldsymbol{\theta}_k + \hat{\boldsymbol{\theta}} = \hat{\boldsymbol{\theta}}$. If $\boldsymbol{\theta}_j > 0$, we get the gradient of Equation 29 as $\boldsymbol{\theta}_j - \mathbf{z}_j + \lambda_j^*$. By making it zero, we obtain $(\boldsymbol{\theta}_{k+1})_j = \mathbf{z}_j - \lambda_j^* > 0$, in which case $\mathbf{z}_j > \lambda_j^*$. If $\boldsymbol{\theta}_j < 0$, we similarly obtain $(\boldsymbol{\theta}_{k+1})_j = \mathbf{z}_j + \lambda_j^* < 0$, in which case $\mathbf{z}_j < -\lambda_j^*$. If $\boldsymbol{\theta}_j = 0$, Equation 29 simply converges and $(\boldsymbol{\theta}_{k+1})_j = 0$, which corresponds with $|\mathbf{z}_j| \leq \lambda_j^*$. Accordingly, we have the following iteration:

$$(\boldsymbol{\theta}_{k+1})_j = \begin{cases} \mathbf{z}_j - \lambda_j^*, & \mathbf{z}_j > \lambda_j^* \\ 0, & |\mathbf{z}_j| \leq \lambda_j^* \\ \mathbf{z}_j + \lambda_j^*, & \mathbf{z}_j < -\lambda_j^* \end{cases} \quad (30)$$

Since \mathbf{z} and $\boldsymbol{\lambda}^*$ are deterministic, Equation 30 is actually a one-off solver. If we set $\lambda_j^* = \sup |\hat{\boldsymbol{\theta}}_j - \bar{\boldsymbol{\theta}}_j|$, for $\boldsymbol{\theta}_j^* > 0$, we have $\boldsymbol{\theta}_j^* = \mathbf{z}_j - \lambda_j^* = \hat{\boldsymbol{\theta}}_j - \sup |\hat{\boldsymbol{\theta}}_j - \bar{\boldsymbol{\theta}}_j| \leq \hat{\boldsymbol{\theta}}_j - |\hat{\boldsymbol{\theta}}_j - \bar{\boldsymbol{\theta}}_j|$. Since $\boldsymbol{\theta}_j^*$ is re-calibrated from $\mathbf{z}_j = \hat{\boldsymbol{\theta}}_j$, $\hat{\boldsymbol{\theta}}_j$ has the same sign as $\boldsymbol{\theta}_j^*$, which implies $\hat{\boldsymbol{\theta}}_j > |\hat{\boldsymbol{\theta}}_j - \bar{\boldsymbol{\theta}}_j|$. Suppose $|\hat{\boldsymbol{\theta}}_j - \bar{\boldsymbol{\theta}}_j| > 1$, which happens frequently in high-dimensional space, we then have $\hat{\boldsymbol{\theta}}_j > 1$. Because $\bar{\boldsymbol{\theta}}_j \leq 1$, $|\hat{\boldsymbol{\theta}}_j - \bar{\boldsymbol{\theta}}_j| = \hat{\boldsymbol{\theta}}_j - \bar{\boldsymbol{\theta}}_j$ holds. Therefore, we have $0 < \boldsymbol{\theta}_j^* \leq \hat{\boldsymbol{\theta}}_j - |\hat{\boldsymbol{\theta}}_j - \bar{\boldsymbol{\theta}}_j| = \bar{\boldsymbol{\theta}}_j \leq 1$, which proves $0 \leq |\boldsymbol{\theta}_j^* - \bar{\boldsymbol{\theta}}_j| < 1$. As such, $|\boldsymbol{\theta}_j^* - \bar{\boldsymbol{\theta}}_j| < 1 < |\hat{\boldsymbol{\theta}}_j - \bar{\boldsymbol{\theta}}_j|$ accordingly holds. Similarly, we derive $|\boldsymbol{\theta}_j^* - \bar{\boldsymbol{\theta}}_j| < 1 < |\hat{\boldsymbol{\theta}}_j - \bar{\boldsymbol{\theta}}_j|$ for $\boldsymbol{\theta}_j^* < 0$. For $\boldsymbol{\theta}_j^* = 0$, $|\boldsymbol{\theta}_j^* - \bar{\boldsymbol{\theta}}_j| = |\bar{\boldsymbol{\theta}}_j| \leq 1 < |\hat{\boldsymbol{\theta}}_j - \bar{\boldsymbol{\theta}}_j|$. In general, we have:

$$\begin{aligned} |\boldsymbol{\theta}_j^* - \bar{\boldsymbol{\theta}}_j| &< |\hat{\boldsymbol{\theta}}_j - \bar{\boldsymbol{\theta}}_j| \\ \text{if } \lambda_j^* &= \sup |\hat{\boldsymbol{\theta}}_j - \bar{\boldsymbol{\theta}}_j| \text{ and } |\hat{\boldsymbol{\theta}}_j - \bar{\boldsymbol{\theta}}_j| > 1 \end{aligned} \quad (31)$$

□

This lemma specifies the suitable regularization weight and the required threshold for utility enhancement in one dimension. On this basis, we prove the superiority of *HDR4ME* with L_1 to the current aggregation in high-dimensional space.

Theorem 3. For any high-dimensional LDP mechanism \mathcal{M} under HDR4ME with L_1 -regularization, the following inequality holds with at least $1 - \int_{-1}^1 \dots \int_{-1}^1 f(\hat{\theta} - \bar{\theta})d(\hat{\theta} - \bar{\theta})$ probability:

$$\|\theta^* - \bar{\theta}\|_2 < \|\hat{\theta} - \bar{\theta}\|_2 \quad (32)$$

where $f(\hat{\theta} - \bar{\theta})$ is obtained from Theorem 1.

Proof. Lemma 4 establishes that $|\theta_j^* - \bar{\theta}_j| < |\hat{\theta}_j - \bar{\theta}_j|$ holds with one certain threshold: $|\hat{\theta}_j - \bar{\theta}_j| > 1$. Theorem 1 derives that $|\hat{\theta}_j - \bar{\theta}_j| > 1$ holds for $\forall j \in [1, d]$ with at least the probability $1 - \int_{-1}^1 \dots \int_{-1}^1 f(\hat{\theta} - \bar{\theta})d(\hat{\theta} - \bar{\theta})$. On this basis,

$$\|\theta^* - \bar{\theta}\|_2 = \sqrt{\sum_{j=1}^d |\theta_j^* - \bar{\theta}_j|^2} < \sqrt{\sum_{j=1}^d |\hat{\theta}_j - \bar{\theta}_j|^2} = \|\hat{\theta} - \bar{\theta}\|_2 \quad (33)$$

□

In general, Theorem 3 derives the least probability for L_1 to enhance utilities in high-dimensional space. Nevertheless, a solver to HDR4ME with L_1 is still required. Applying $z = \hat{\theta}$ and $(\theta_{k+1})_j = \theta_j^*$ to Equation 30, we have:

$$\theta_j^* = \begin{cases} \hat{\theta}_j - \lambda_j^*, & \hat{\theta}_j > \lambda_j^* \\ 0, & |\hat{\theta}_j| \leq \lambda_j^* \\ \hat{\theta}_j + \lambda_j^*, & \hat{\theta}_j < -\lambda_j^* \end{cases} \quad (34)$$

Equation 34 is a one-off, non-iterative solver for HDR4ME with L_1 , which simply re-calibrates the estimated mean to get the enhanced mean. As such, the data collector can enhance utilities without bearing extra computational burden.

HDR4ME with L_2 -regularization. This re-calibration can obtain much deviation $\|\hat{\theta} - \bar{\theta}\|_2$ by scale reduction. To achieve this, λ^* must satisfy the following condition.

Lemma 5. HDR4ME with L_2 -regularization can improve accuracy in j -th dimension if

$$\lambda_j^* = \sup \frac{\hat{\theta}_j - \bar{\theta}_j}{2\lambda_j^*} \text{ and } |\hat{\theta}_j - \bar{\theta}_j| > 2 \quad (35)$$

where $\hat{\theta}_j - \bar{\theta}_j$ is obtained from Lemma 2 or Lemma 3, and $\bar{\theta}_j$ can select the mean of the normal distribution that approximates $\hat{\theta}_j - \bar{\theta}_j$ in our framework.

Proof. Following Equation 27, we add L_2 -regularization term into the iteration:

$$\theta_{k+1} = \arg \min_{\theta} \frac{1}{2} \|\theta - (\theta_k - \nabla \mathcal{L}(\theta_k))\|_2^2 + \|\lambda^* \circ \theta\|_2^2 \quad (36)$$

Since each dimension is perturbed independently, we have the following solution for each dimension:

$$(\theta_{k+1})_j = \arg \min_{\theta_j} \frac{1}{2} |\theta_j - ((\theta_k)_j - \nabla \mathcal{L}(\theta_k)_j)|_2^2 + |\lambda_j^* \theta_j|^2 \quad (37)$$

where $z = \theta_k - \nabla \mathcal{L}(\theta_k) = \hat{\theta}$. Note that Equation 37 is differentiable. Applying 0 to the derivative of Equation 37,

we have $\theta_j^* = \frac{\hat{\theta}_j}{2\lambda_j^* + 1}$. If $\lambda_j^* = \sup \frac{\hat{\theta}_j - \bar{\theta}_j}{2\lambda_j^*}$, our framework implies $\lambda_j^* > 0$. Then, we derive:

$$|\theta_j^*| = \left| \frac{\hat{\theta}_j}{2\lambda_j^* + 1} \right| = \left| \frac{\hat{\theta}_j}{\sup \frac{\hat{\theta}_j - \bar{\theta}_j}{\lambda_j^*} + 1} \right| \leq \left| \frac{\hat{\theta}_j}{\frac{\hat{\theta}_j - \bar{\theta}_j}{\lambda_j^*} + 1} \right| = |\bar{\theta}_j| \quad (38)$$

Therefore, we have $0 \leq |\theta_j^*| \leq |\bar{\theta}_j| \leq 1$, which implies $0 \leq |\theta_j^* - \bar{\theta}_j| \leq 2$. Namely, we have:

$$\begin{aligned} |\theta_j^* - \bar{\theta}_j| &< |\hat{\theta}_j - \bar{\theta}_j| \\ \text{if } \lambda_j^* = \sup \frac{\hat{\theta}_j - \bar{\theta}_j}{2\lambda_j^*} \text{ and } |\hat{\theta}_j - \bar{\theta}_j| &> 2 \end{aligned} \quad (39)$$

□

Now that this lemma specifies the suitable regularization weight and the required threshold for utility enhancement in one dimension, we further prove the superiority of HDR4ME with L_2 to the current aggregation in high-dimensional space.

Theorem 4. For any high-dimensional LDP mechanism \mathcal{M} under HDR4ME with L_2 -regularization, the following inequality holds with at least $1 - \int_{-2}^2 \dots \int_{-2}^2 f(\hat{\theta} - \bar{\theta})d(\hat{\theta} - \bar{\theta})$ probability:

$$\|\theta^* - \bar{\theta}\|_2 < \|\hat{\theta} - \bar{\theta}\|_2 \quad (40)$$

where $f(\hat{\theta} - \bar{\theta})$ is obtained from Theorem 1.

Proof. Equation 31 in Lemma 5 derives that $|\theta_j^* - \bar{\theta}_j| < |\hat{\theta}_j - \bar{\theta}_j|$ holds with one certain threshold: $|\hat{\theta}_j - \bar{\theta}_j| > 2$. Theorem 1 derives that $|\hat{\theta}_j - \bar{\theta}_j| > 2$ holds for $\forall j \in [1, d]$ with at least the probability $1 - \int_{-2}^2 \dots \int_{-2}^2 f(\hat{\theta} - \bar{\theta})d(\hat{\theta} - \bar{\theta})$. On this basis,

$$\|\theta^* - \bar{\theta}\|_2 = \sqrt{\sum_{j=1}^d |\theta_j^* - \bar{\theta}_j|^2} < \sqrt{\sum_{j=1}^d |\hat{\theta}_j - \bar{\theta}_j|^2} = \|\hat{\theta} - \bar{\theta}\|_2 \quad (41)$$

□

With our framework, Theorem 4 derives the least probability for L_2 to enhance utilities in high-dimensional space, in which case the enhanced mean is always better than estimated mean. To solve HDR4ME with L_2 , we compute the derivative of Equation 37 and set it to zero:

$$\theta_j^* = \theta_k - \nabla \mathcal{L}(\theta_k) = \frac{\hat{\theta}_j}{2\lambda_j^* + 1} \quad (42)$$

Similarly, the above is also a one-off, non-iterative solver for HDR4ME with L_2 , which does not increase the computational burden of the data collector.

As a final note, both types of HDR4ME are designed for “high-dimensional” space only. In such a space, the useful statistics are flooded by much larger noise, which provides us room to make utility enhancement. If the number of dimensions is not high or the collective privacy budget is rather large, which generally means that the threshold for

either regularization to enhance utilities is not reached, our re-calibration can be harmful.

C. High-dimensional Re-calibration for Frequency Estimation

For various LDP mechanisms, high-dimensional frequency estimation is never sufficiently discussed, especially when some mechanisms claim to be applicable to both mean and frequency estimations [11], [37]. As such, we also generalize our re-calibration to frequency estimation. Note that any categorical value can be mapped into a binary vector with *histogram encoding* [37]. Suppose there are d categorical dimensions and $v_j (1 \leq j \leq d)$ categories in each dimension, any categorical value in j -th dimension $t_{ij} (1 \leq i \leq r_j)$ can be encoded to a v_j -entry vector $(0.0, 0.0, \dots, 1.0, \dots, 0.0)^T$ with only the t_{ij} -th entry to be 1.0. As such, each of d categorical dimensions is expanded to one v_j -dimensional numerical space. Note that each entry of encoded vectors ranges from $[0, 1]$. If each user reports m dimensions of her perturbed data to the data collector, the collective ϵ -LDP can be guaranteed by applying $\frac{\epsilon}{2m}$ to each entry of vectors [37] regardless of LDP mechanisms. As such, the data collector receives $r_j v_j$ -entry perturbed vectors in j -th dimension. Since each entry corresponds with one certain categorical value, the mean of r_j perturbed vectors corresponds with the estimated frequencies in j -th dimension, with each entry of the mean to be the frequency of each categorical value. In general, we can convert one d -dimensional frequency estimation to d high-dimensional mean estimation tasks. On this basis, both our framework and re-calibration protocol can further apply.

VI. EXPERIMENTAL EVALUATION

To verify both the analytical framework and the re-calibration protocol, we conduct experiments under a real dataset COV-19¹ and three synthetically distributed datasets, namely Gaussian, Poisson and Uniform. The following are some descriptions of four datasets:

- 1) The COV-19 dataset consists of 150,000 users and 750 dimensions, where each dimension has high correlations with others.
- 2) The Gaussian dataset consists of tunable users and dimensions. The standard deviation of all dimensions is set to $1/16$. 10% dimensions have their mathematical expectations $\mu = 0.9$ whereas the other 90% have $\mu = 0$.
- 3) The Poisson dataset consists of 150,000 users and 300 dimensions, where each dimension follows a Poisson distribution with a random expectation from 1 to 99.
- 4) The Uniform dataset consists of tunable users and dimensions.

The aims of our experiments are twofold. First, we confirm the effectiveness of our analytical framework, namely, $\hat{\theta}_j - \bar{\theta}_j$ can be approximated with one certain Gaussian distribution. Second, we compare the performances of *HDR4ME* on top of the aggregation results of three state-of-the-art LDP mechanisms, i.e., Laplace [13], Piecewise [11], and Square wave

¹<https://www.kaggle.com/allen-institute-for-ai/CORD-19-research-challenge>

[12]. Each dimension is normalized into $[-1, 1]$, and each experiment is repeated 100 times to obtain the averaged result unless otherwise indicated. All our experiments are implemented in MATLAB on a laptop computer with Intel Core i7-10750H 2.59 GHz CPU, 32G RAM on Windows 10 operation system.

In the first set of experiments, for a start, we use Uniform dataset to verify the effectiveness of our analytical framework. In specific, we set 200,000 users and 5,000 dimensions. For each user, they send 50 dimensions of her perturbed tuples to the data collector. To ensure generality, we conduct experiments on Laplace, Piecewise and Square wave, respectively. Each experiment is iterated 1,000 times, and we collect the means of 1,000 times in the first dimension. Given the collective privacy budget $\epsilon = 1$, Fig. 2 shows how our framework models the means from experiments. In each sub-figure, the blue line is the pdf of the deviations from our framework while the orange squares are the pdf estimate from experiments. In all three mechanisms, our framework effectively approximates experimental results. Recall that we provide a case study in Section IV-C to benchmark Piecewise and Square wave. To support the benchmark results, we discretize the Uniform dataset and conduct experiments in Fig. 3. In both mechanisms, the pdf functions computed in our case study perfectly model the experimental results, which confirms the effectiveness of the benchmark by our framework.

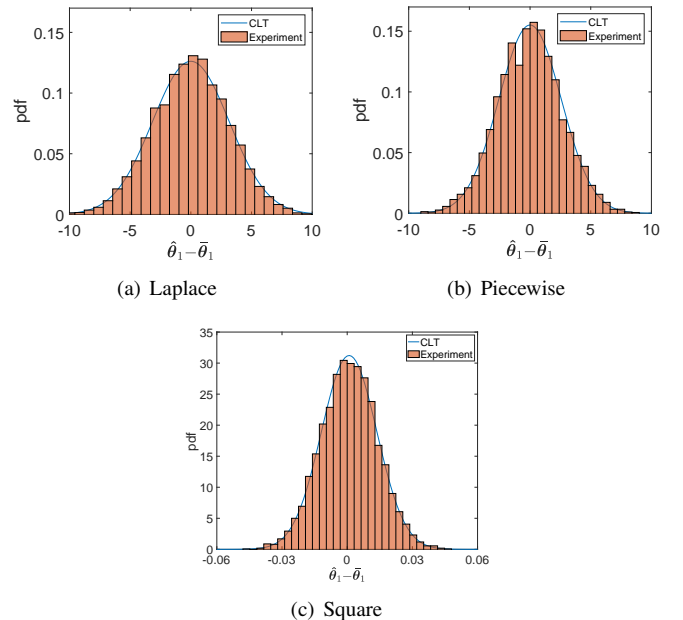


Fig. 2. Analysis vs. experimental results on Uniform dataset ($d=5,000$).

In the second set of experiments, we evaluate impacts of different LDP mechanisms, privacy budget and dimensionality on our re-calibration protocol. In particular, ϵ is varied in the set $\{0.1, 0.2, 0.4, 0.8, 1.6, 3.2\}$ for Laplace and Piecewise while in the set $\{0.1, 10, 100, 500, 1000, 5000\}$ for Square wave. We set a different range of ϵ for Square wave because its utility hardly varies with small ϵ [12]. To test the limit of our

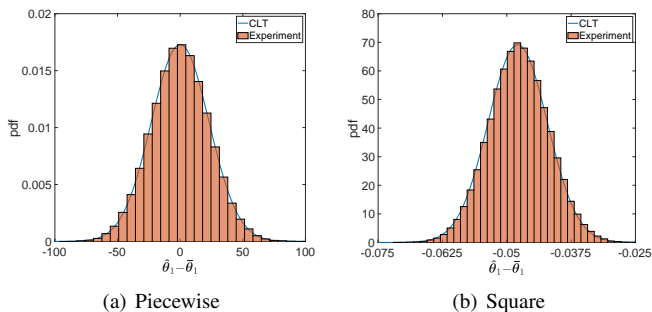


Fig. 3. Analysis vs. experimental results in our case study.

protocol, each user sends all dimensions of her perturbed tuple to the data collector. Accordingly, ϵ is partitioned according to respective dimensions. Figs. 4(a)-(c) plot MSE results with respect to ϵ under the Gaussian dataset, where users and dimensions are respectively set 100,000 and 100. Overall, both L_1 - and L_2 -regularization enhance the aggregation accuracy in all three LDP mechanisms. In contrast to L_1 , the MSE of L_2 decreases at a slower rate as ϵ increases, mostly because the regularization weights of L_2 become so large under 100 dimensions that any change of ϵ has a minor impact on the regularized results. Although our protocol mostly increases the utilities, there exist some expectations. In Square wave, L_2 is outperformed by the current aggregation if $\epsilon = 5,000$ while L_1 tends to get the same results as the current aggregation regardless of ϵ . It is noteworthy, however, that MSE results of both L_1 and L_2 may become worse than the current aggregation. In essence, if the deviation of the LDP mechanism does not satisfy the threshold in either Lemma 4 or Lemma 5, our re-calibration can be harmful. In this sense, regularization should not be heavily involved or even involved at all. Note that Square wave mechanism perturbs original data from $[0, 1]$ to $[-b, b + 1]$, where $b \rightarrow \frac{1}{2}$ if $\epsilon \rightarrow 0$ while $b \rightarrow 0$ if $\epsilon \rightarrow +\infty$ [12]. With so concentrated perturbation, its deviation in each dimension can be so small that the threshold of either regularization is not satisfied. That is why L_2 could make its utility even worse. In contrast, our protocol successfully enhances utilities of Laplace and Piecewise because their perturbations are rather large in high-dimensional space.

Next, we implement Poisson dataset (150,000 users, 300 dimensions), Uniform dataset (120,000 users, 500 dimensions) and COV-19 dataset (150,000 users, 750 dimensions) to repeat the utility enhancement experiment. ϵ is partitioned according to respective dimensions. Figs. 4(d)-(f), (g)-(i) and (j)-(l) show respective MSE results with regard to different datasets. In specific, Figs. 4(f), (i) and (l) confirm that our protocol is not suitable for Square wave whose deviation is already small enough in high-dimensional space while other figures indicate that both L_1 and L_2 enhance utilities of Laplace and Piecewise. Notably, MSE results of L_2 in Figs. 4(g), (h), (j) and (k) almost remain unchanged. Due to the extremely high dimensionality (e.g. $d=500$ and $d=750$), regularization weights of L_2 become so large that each entry of the enhanced mean is nearly zero. In this sense, MSE results of L_2 hardly change.

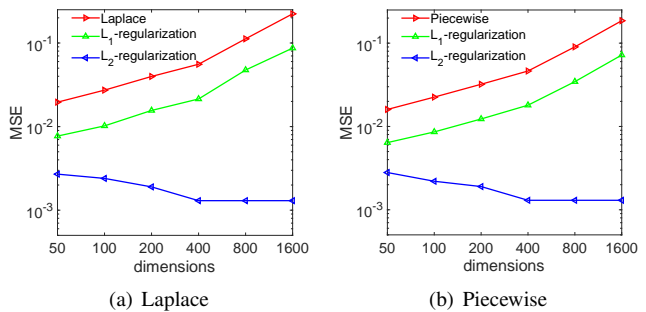


Fig. 5. MSE on COV-19 dataset with various dimensions.

In the third sets of experiments, we continue to evaluate the impact of dimensionality on our protocols under the COV-19 dataset, where ϵ is set 0.8, and the dimensionality varies in the set $\{50, 100, 200, 400, 800, 1600\}$. Since the dataset with dimensionality like 1600 is very hard to find, we randomly sample some dimensions from COV-19 dataset to make up. Fig. 5 shows MSE results of the Laplace and Piecewise, where our protocol enhances the current aggregation regardless of dimensionality. In particular, L_2 provides even better utilities as dimensionality increases, as opposed to both the current aggregation and L_1 . The rationale is similar as above — the regularization weights of L_2 are much larger than those of L_1 as dimensionality increases, which reduces the scale of perturbation more effectively. In this sense, MSE results of L_2 in both mechanisms decrease as dimensionality increases (e.g. $d = 50, 100, 200$). As the dimensionality becomes extremely large (e.g. $d = 400, 800, 1600$), regularization weights of L_2 become so large that each entry of enhanced mean is nearly zero. In this sense, MSE results of L_2 hardly change.

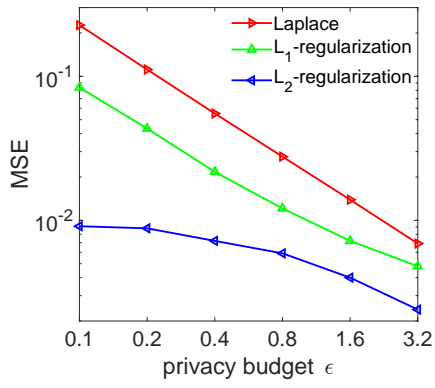
VII. CONCLUSION

This work investigates utilities of mean estimation by LDP mechanisms in high-dimensional space. In terms of the deviation between the estimated mean and the true mean, we propose an analytical framework to evaluate any LDP mechanism. This framework provides closed-form evaluation on individual LDP mechanism. In addition, we propose *HDR4ME* to re-calibrate the aggregation results from these LDP mechanisms to further enhance their utilities in high-dimensional space. Through theoretical analysis and extensive experiments, we confirm the generality and effectiveness of our analytical framework and re-calibration protocol under various datasets and parameter settings.

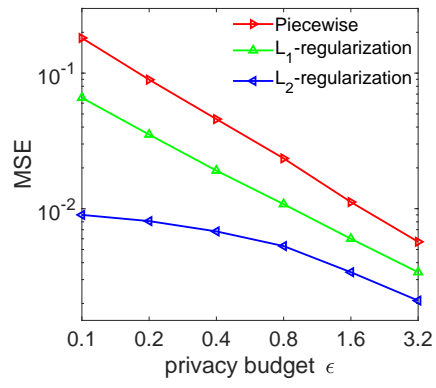
For the future work, we plan to extend our work to other data type, e.g., set-value data, and more data analysis tasks, e.g., other statistics estimation and machine learning models.

ACKNOWLEDGEMENTS

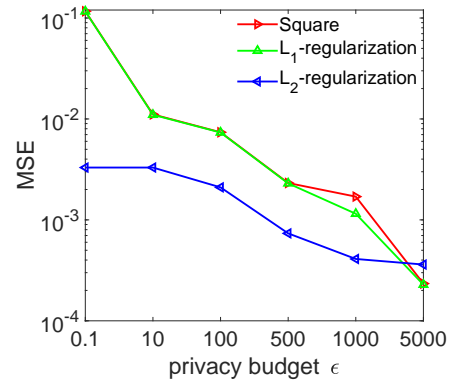
This work was supported by National Natural Science Foundation of China (Grant No: 62072390 and 62102334), the Research Grants Council, Hong Kong SAR, China (Grant No: 15222118, 15218919, 15203120, 15226221 and 15225921), and Centre for Advances in Reliability and Safety (CAiRS) admitted under AiR@InnoHK Research Cluster.



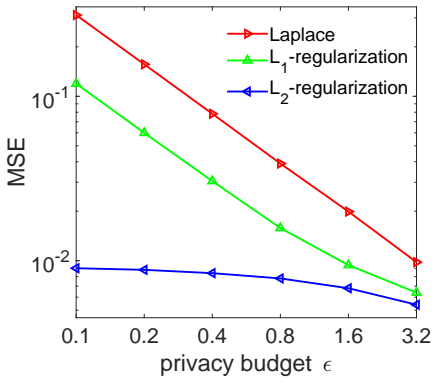
(a) Laplace on Gaussian ($d = 100$)



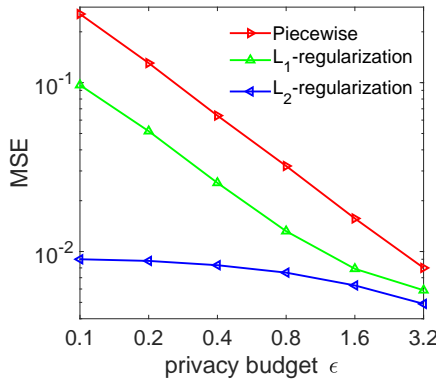
(b) Piecewise on Gaussian ($d = 100$)



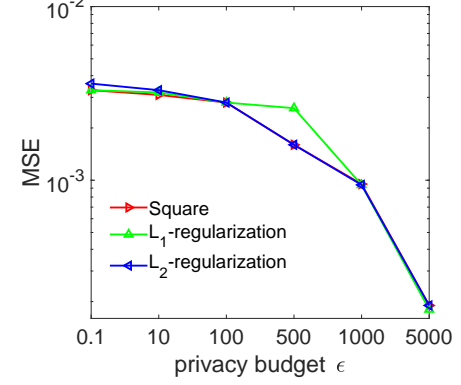
(c) Square on Gaussian ($d = 100$)



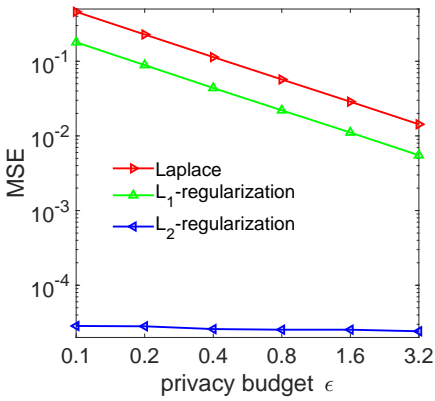
(d) Laplace on Poisson ($d = 300$)



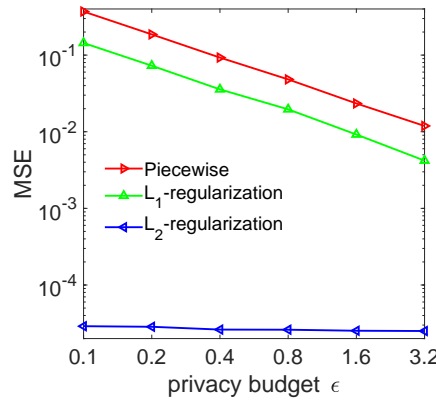
(e) Piecewise on Poisson ($d = 300$)



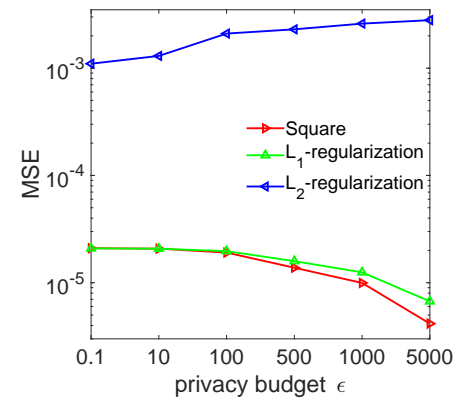
(f) Square on Poisson ($d = 300$)



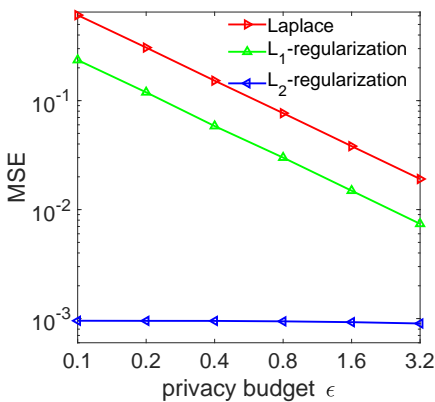
(g) Laplace on Uniform ($d = 500$)



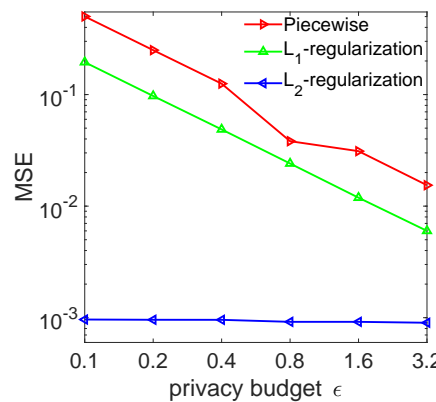
(h) Piecewise on Uniform ($d = 500$)



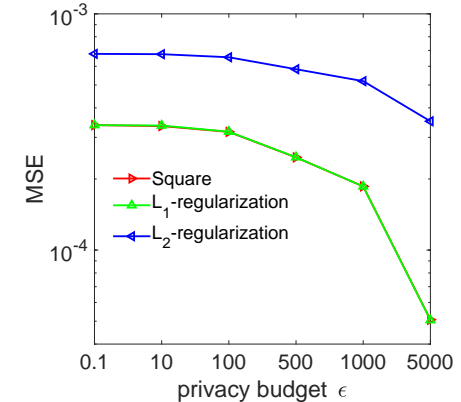
(i) Square on Uniform ($d = 500$)



(j) Laplace on COV-19 ($d = 750$)



(k) Piecewise on COV-19 ($d = 750$)



(l) Square on COV-19 ($d = 750$)

Fig. 4. MSE on various datasets and dimensions

REFERENCES

- [1] M. Barbosa, S. B. Mokhtar, P. Felber, F. Maia, M. Matos, R. Oliveira, E. Riviere, V. Schiavoni, and S. Voulgaris, "Safethings: Data security by design in the iot," in *EDCC*, 2017, pp. 117–120.
- [2] J. Liu, C. Zhang, and Y. Fang, "Epic: A differential privacy framework to defend smart homes against internet traffic analysis," *IEEE Internet of Things Journal*, vol. 5, no. 2, pp. 1206–1217, 2018.
- [3] S. Ghayyur, Y. Chen, R. Yus, A. Machanavajjhala, M. Hay, G. Miklau, and S. Mehrotra, "Iot-detective: Analyzing iot data under differential privacy," in *SIGMOD*, 2018, pp. 1725–1728.
- [4] Z. Liu, Z. Huang, H. Lyu, Z. Li, W. Liu *et al.*, "Dynapro: Dynamic wireless sensor network data protection algorithm in iot via differential privacy," *IEEE Access*, vol. 7, pp. 167 754–167 765, 2019.
- [5] I. Psychoula, L. Chen, and O. Amft, "Privacy risk awareness in wearables and the internet of things," *IEEE Pervasive Computing*, vol. 19, no. 3, pp. 60–66, 2020.
- [6] S. Raskhodnikova, A. Smith, H. K. Lee, K. Nissim, and S. P. Kavitswanathan, "What can we learn privately," in *FOCS*, 2008, pp. 531–540.
- [7] J. C. Duchi, M. I. Jordan, and M. J. Wainwright, "Local privacy and statistical minimax rates," in *FOCS*. IEEE, 2013, pp. 429–438.
- [8] Q. Ye and H. Hu, "Local differential privacy: Tools, challenges, and opportunities," in *WISE*. Springer, 2020, pp. 13–23.
- [9] J. Soria-Comas and J. Domingo-Ferrer, "Optimal data-independent noise for differential privacy," *Information Sciences*, vol. 250, pp. 200–214, 2013.
- [10] Q. Geng, P. Kairouz, S. Oh, and P. Viswanath, "The staircase mechanism in differential privacy," *IEEE Journal of Selected Topics in Signal Processing*, vol. 9, no. 7, pp. 1176–1184, 2015.
- [11] N. Wang, X. Xiao, Y. Yang, J. Zhao, S. C. Hui, H. Shin, J. Shin, and G. Yu, "Collecting and analyzing multidimensional data with local differential privacy," in *ICDE*. IEEE, 2019, pp. 638–649.
- [12] Z. Li, T. Wang, M. Lopuhaä-Zwakenberg, N. Li, and B. Škoric, "Estimating numerical distributions under local differential privacy," in *SIGMOD*, 2020, pp. 621–635.
- [13] C. Dwork, F. McSherry, K. Nissim, and A. Smith, "Calibrating noise to sensitivity in private data analysis," in *Theory of Cryptography*, S. Halevi and T. Rabin, Eds. Berlin, Heidelberg: Springer Berlin Heidelberg, 2006, pp. 265–284.
- [14] A. Evfimievski, J. Gehrke, and R. Srikant, "Limiting privacy breaches in privacy preserving data mining," in *PODS*, 2003, pp. 211–222.
- [15] T. Wang, N. Li, and S. Jha, "Locally differentially private frequent itemset mining," in *S&P*. IEEE, 2018, pp. 127–143.
- [16] G. Cormode, T. Kulkarni, and D. Srivastava, "Marginal release under local differential privacy," in *SIGMOD*. ACM, 2018, pp. 131–146.
- [17] Z. Zhang, T. Wang, N. Li, S. He, and J. Chen, "CALM: Consistent adaptive local marginal for marginal release under local differential privacy," in *CCS*. ACM, 2018, pp. 212–229.
- [18] Q. Ye, H. Hu, N. Li, X. Meng, H. Zheng, and H. Yan, "Beyond value perturbation: Local differential privacy in the temporal setting," in *INFOCOM*. IEEE, 2021, pp. 1–10.
- [19] H. Sun, X. Xiao, I. Khalil, Y. Yang, Z. Qin, H. W. Wang, and T. Yu, "Analyzing subgraph statistics from extended local views with decentralized differential privacy," in *CCS*. ACM, 2019, pp. 703–717.
- [20] Q. Ye, H. Hu, M. H. Au, X. Meng, and X. Xiao, "Towards locally differentially private generic graph metric estimation," in *ICDE*. IEEE, 2020, pp. 1922–1925.
- [21] —, "LF-GDPR: graph metric estimation with local differential privacy," *IEEE Transactions on Knowledge and Data Engineering (TKDE)*, 2020.
- [22] Q. Ye, H. Hu, X. Meng, and H. Zheng, "PrivKV: Key-value data collection with local differential privacy," in *S&P*. IEEE, 2019, pp. 317–331.
- [23] X. Gu, M. Li, Y. Cheng, L. Xiong, and Y. Cao, "PCKV: locally differentially private correlated key-value data collection with optimized utility," in *USENIX Security Symposium*, 2020.
- [24] Q. Ye, H. Hu, X. Meng, H. Zheng, K. Huang, C. Fang, and J. Shi, "PrivKVM*: Revisiting key-value statistics estimation with local differential privacy," *IEEE Transactions on Dependable and Secure Computing*, 2021.
- [25] H. Zheng, Q. Ye, H. Hu, C. Fang, and J. Shi, "BDPL: A boundary differentially private layer against machine learning model extraction attacks," in *ESORICS*. Springer, 2019, pp. 66–83.
- [26] —, "Protecting decision boundary of machine learning model with differentially private perturbation," *IEEE Transactions on Dependable and Secure Computing*, 2020.
- [27] J. C. Duchi, M. I. Jordan, and M. J. Wainwright, "Minimax optimal procedures for locally private estimation," *Journal of the American Statistical Association*, vol. 113, no. 521, pp. 182–201, 2018.
- [28] X. Ren, C.-M. Yu, W. Yu, S. Yang, X. Yang, J. A. McCann, and S. Y. Philip, "Lopub: High-dimensional crowdsourced data publication with local differential privacy," *IEEE Transactions on Information Forensics and Security*, vol. 13, no. 9, pp. 2151–2166, 2018.
- [29] J. Ge, Z. Wang, M. Wang, and H. Liu, "Minimax-optimal privacy-preserving sparse pca in distributed systems," in *International Conference on Artificial Intelligence and Statistics, AISTATS 2018*, 2018.
- [30] D. Wang and J. Xu, "Principal component analysis in the local differential privacy model," *Theoretical Computer Science*, vol. 809, pp. 296–312, 2020.
- [31] R. Bassily, "Linear queries estimation with local differential privacy," in *The 22nd International Conference on Artificial Intelligence and Statistics*. PMLR, 2019, pp. 721–729.
- [32] K. Chatzikokolakis, M. E. Andrés, N. E. Bordenabe, and C. Palamidessi, "Broadening the scope of differential privacy using metrics," in *International Symposium on Privacy Enhancing Technologies Symposium*. Springer, 2013, pp. 82–102.
- [33] M. Alvim, K. Chatzikokolakis, C. Palamidessi, and A. Pazzi, "Local differential privacy on metric spaces: optimizing the trade-off with utility," in *CSF*. IEEE, 2018, pp. 262–267.
- [34] X. Li, C. Luo, P. Liu, and L.-e. Wang, "Information entropy differential privacy: A differential privacy protection data method based on rough set theory," in *2019 IEEE Intl Conf on Dependable, Autonomic and Secure Computing, Intl Conf on Pervasive Intelligence and Computing, Intl Conf on Cloud and Big Data Computing, Intl Conf on Cyber Science and Technology Congress*. IEEE, 2019, pp. 918–923.
- [35] R. Du, Q. Ye, Y. Fu, and H. Hu, "Collecting high-dimensional and correlation-constrained data with local differential privacy," in *SECON*. IEEE, 2021, pp. 1–9.
- [36] T. T. Nguyễn, X. Xiao, Y. Yang, S. C. Hui, H. Shin, and J. Shin, "Collecting and analyzing data from smart device users with local differential privacy," *arXiv preprint arXiv:1606.05053*, 2016.
- [37] T. Wang, J. Blocki, N. Li, and S. Jha, "Locally differentially private protocols for frequency estimation," in *USENIX Security Symposium*, 2017, pp. 729–745.
- [38] S. Kotz, T. Kozubowski, and K. Podgórski, *The Laplace distribution and generalizations: a revisit with applications to communications, economics, engineering, and finance*. Springer Science & Business Media, 2001, no. 183.
- [39] J. G. Shanthikumar and U. Sumita, "A central limit theorem for random sums of random variables," *Operations Research Letters*, vol. 3, no. 3, pp. 153–155, 1984.
- [40] H. Fischer, *A history of the central limit theorem. From classical to modern probability theory*, 01 2011.
- [41] D. S. Lemons, "An introduction to stochastic processes in physics," 2003.
- [42] V. Y. Korolev and I. G. Shevtsova, "On the upper bound for the absolute constant in the berry–esseen inequality," *Theory of Probability & Its Applications*, vol. 54, no. 4, pp. 638–658, 2010.
- [43] S. Boyd and L. Vandenberghe, *Convex Optimization*. Cambridge University Press, 2004.
- [44] P. Bühlmann and S. Van De Geer, *Statistics for high-dimensional data: methods, theory and applications*. Springer Science & Business Media, 2011.
- [45] P. O. Hoyer, "Non-negative matrix factorization with sparseness constraints," *Journal of machine learning research*, vol. 5, no. 9, 2004.
- [46] S. N. Negahban, P. Ravikumar, M. J. Wainwright, B. Yu *et al.*, "A unified framework for high-dimensional analysis of m -estimators with decomposable regularizers," *Statistical science*, vol. 27, no. 4, pp. 538–557, 2012.
- [47] R. Tibshirani, "Regression shrinkage and selection via the lasso," *Journal of the Royal Statistical Society: Series B (Methodological)*, vol. 58, no. 1, pp. 267–288, 1996.
- [48] A. Nitanda, "Stochastic proximal gradient descent with acceleration techniques," *NIPS*, vol. 27, pp. 1574–1582, 2014.
- [49] H. Li and Z. Lin, "Accelerated proximal gradient methods for nonconvex programming," *NIPS*, vol. 28, pp. 379–387, 2015.